

4-18-2011

Nonadiabatic Generation of a Pure Spin Current in a One-Dimensional Quantum Ring with Spin-Orbit Interaction

Marian Nita

National Institute of Materials Physics

D C. Marinescu

Clemson University, dcm@clemson.edu

Andrei Manolescu

Reykjavik University

Vidar Gudmundsson

University of Iceland

Follow this and additional works at: https://tigerprints.clemson.edu/physastro_pubs

 Part of the [Astrophysics and Astronomy Commons](#)

Recommended Citation

Please use publisher's recommended citation.

This Article is brought to you for free and open access by the Physics and Astronomy at TigerPrints. It has been accepted for inclusion in Publications by an authorized administrator of TigerPrints. For more information, please contact kokeefe@clemson.edu.

Nonadiabatic generation of a pure spin current in a one-dimensional quantum ring with spin-orbit interaction

Marian Niță,¹ D. C. Marinescu,² Andrei Manolescu,³ and Vidar Gudmundsson⁴

¹*National Institute of Materials Physics, P.O. Box MG-7, Bucharest-Magurele, Romania*

²*Department of Physics and Astronomy, Clemson University, Clemson, South Carolina 29634, USA*

³*School of Science and Engineering, Reykjavik University, Menntavegur 1, IS-101 Reykjavik, Iceland*

⁴*Science Institute, University of Iceland, Dunhaga 3, IS-107 Reykjavik, Iceland*

(Received 14 February 2011; revised manuscript received 3 March 2011; published 18 April 2011)

We demonstrate the theoretical possibility of obtaining a pure spin current in a 1D ring with spin-orbit interaction by irradiation with a nonadiabatic, two-component terahertz laser pulse, whose spatial asymmetry is reflected by an internal phase difference ϕ . The solutions of the equation of motion for the density operator are obtained for a spin-orbit coupling linear in the electron momentum (Rashba) and they are used to calculate the time-dependent charge and spin currents. We find that there are critical values of ϕ at which the charge current disappears, while the spin current reaches a maximum or a minimum value.

DOI: [10.1103/PhysRevB.83.155427](https://doi.org/10.1103/PhysRevB.83.155427)

PACS number(s): 73.23.Ra, 71.70.Ej, 72.25.Dc, 73.21.Hb

I. INTRODUCTION

Obtaining and controlling spin currents in solid structures has been one of the most important goals of spintronics research. In the recent past the focus of this endeavor has been on the creative use of the spin-orbit interaction (SOI) that appears in systems with broken inversion symmetry, be that via confinement (Rashba)¹ or in the bulk (Dresselhaus).² The well-known properties of quasi-one-dimensional rings to support persistent charge currents³⁻⁵ made them particularly appealing for spin transport exploration. The underlying physical phenomenon leading to the creation of persistent charge currents is the imbalance in the left/right charge carrying states realized, initially, in the presence of a magnetic flux threaded through the center of the ring. In a similar theoretical setup the existence of persistent spin currents was obtained in the presence of SOI,⁶⁻⁸ when electron-electron interaction is neglected. Both analytical⁶ and numerical results,⁸ point out that in the presence of a magnetic flux the charge and spin currents in the rings are simultaneously present. Theoretical proposals for obtaining pure spin currents focused on either hybrid ring systems⁹ or in rings with an odd number of electrons.¹⁰

In this paper we revisit this problem from the perspective of creating persistent charge and spin current by *nonadiabatic* methods. As before, the original exploration of such ideas was focused on the generation of charge currents by various mechanisms able to produce an imbalance between left/right momentum-carrying states.¹¹⁻¹³ In particular, in this work we are concerned with the application of an ultrashort, terahertz frequency laser pulse, having a spatial asymmetry expressed through an internal phase difference angle ϕ . The efficiency of this method for creating persistent charge currents has been explored in Refs. 13 and 14. Its extension to a ring endowed with SOI is discussed below. As we demonstrate, the interplay between the spin-orbit coupling that rotates the electron spin around the ring and the spatial asymmetry of the external excitation generates favorable conditions where the charge current disappears, while the spin current reaches a maximum or a minimum level. For both a dipolar and a quadrupolar perturbation we can find the critical values of the out-of-phase angle ϕ for which this situation occurs.

II. THE RING MODEL

We consider a one-dimensional (1D) quantum ring of radius r_0 containing few electrons, endowed with a Rashba interaction, linear in the electron momentum. In a discrete representation the ring is reduced to N sites (points) distributed on a circle whose angular coordinates are given by $\theta_n = 2n\pi/N$ with $n = 1, 2, \dots, N$ the site index. The Hamiltonian describing the noninteracting electrons is written in terms of the creation and annihilation operators $c_{n\sigma}^\dagger$ and $c_{n,\sigma}$ associated with the single-particle states $|n\sigma\rangle$, where $\sigma = \pm 1$ is the spin index. This Hamiltonian has been extensively discussed in literature,^{6-8,15} so here we will write it directly:

$$H = V \left\{ 2 \sum_{n,\sigma} c_{n\sigma}^\dagger c_{n\sigma} - \sum_{n,\sigma} [c_{n\sigma}^\dagger c_{n+1\sigma} + c_{n\sigma}^\dagger c_{n-1\sigma}] \right\} - \left\{ i V_\alpha \sum_{n,\sigma,\sigma'} [\sigma_r(\theta_{n,n+1})]_{\sigma\sigma'} c_{n\sigma}^\dagger c_{n+1\sigma'} + \text{H.c.} \right\}. \quad (1)$$

The two energy scales of the problem are set by the hopping matrix element $V = \hbar^2/2m^*a^2$ and by the Rashba energy $V_\alpha = \alpha/2a$, where m^* is the effective electron mass, $a = 2\pi r_0/N$ is the discretization constant, and α is the Rashba spin-orbit coupling strength. The spin operator $\sigma_r(\theta)$ introduced in Eq. (1) represents the local orientation of the electron spin along the radius of the ring and is given by a linear combination of the Pauli operators σ_x, σ_y written for the azimuthal coordinate $\theta_{n,n+1} = (\theta_n + \theta_{n+1})/2$,

$$\sigma_r(\theta_{n,n+1}) = \sigma_x \cos \theta_{n,n+1} + \sigma_y \sin \theta_{n,n+1}. \quad (2)$$

The energy spectrum of the Hamiltonian, calculated for an even number of sites ($N = 20$) is shown in Fig. 1 for $V_\alpha = 0$ and for $V_\alpha = 0.86$ (units of V). The split realized by the SOI can be seen in Fig. 1(b) and it is described by the two sets of eigenvalues E_{l+} (right branch) and E_{l-} (left branch), with

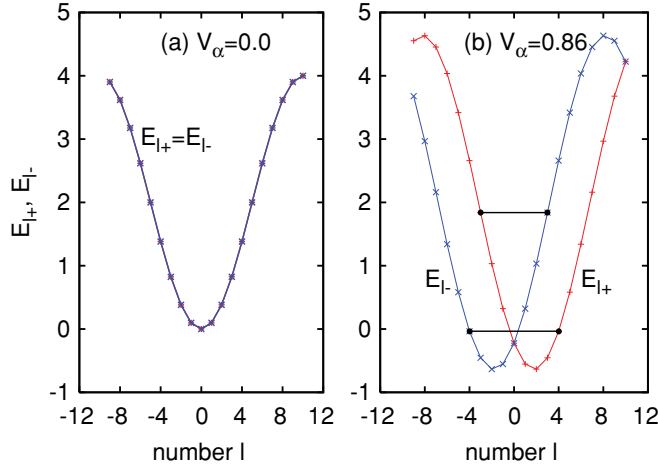


FIG. 1. (Color online) The eigenvalues E_{l+} and E_{l-} of the 1D quantum ring with $N = 20$ points vs quantum number l . The spectrum is discrete and the eigenvalues are represented by the points. The lines connecting the points are only for guiding the eye. In panel (a), in the absence of the SOI ($V_\alpha = 0$), the two branches coincide, i.e., $E_{l+} = E_{l-} = \epsilon_l$. In panel (b), in the presence of the SOI ($V_\alpha = 0.86$), the two branches split, but $E_{l+} = E_{-l-}$ such that all states are double degenerate. For example, the two horizontal lines show that $E_{3-} = E_{-3+} = 1.839$ and $E_{4+} = E_{-4-} = -0.035$. The energy unit is $V = \hbar^2/2m^*a^2$.

$l = 0, \pm 1, \pm 2, \dots, \pm (N/2 - 1), N/2$. The eigenvalues are

$$E_{l\pm} = \frac{\epsilon_l + \epsilon_{l\pm 1}}{2} + \frac{\epsilon_l - \epsilon_{l\pm 1}}{2} \sqrt{1 + \tan^2 2\theta_\alpha}, \quad (3)$$

where $\epsilon_l = 2V - 2V \cos(2\pi l/N)$ are the degenerate eigenvalues in the absence of SOI and θ_α is a special angle given by

$$\tan 2\theta_\alpha = \frac{V_\alpha}{V \sin(\Delta\theta/2)}, \quad (4)$$

where $\Delta\theta = 2\pi/N$. In the continuous limit $N \rightarrow \infty$ or $a \rightarrow 0$ one obtains the form $\tan 2\theta_\alpha = 2m^*r_0\alpha/\hbar^2$ for the continuous model.⁶ The states with energies E_{l+} have the spin pointing along a direction tilted at an angle $2\theta_\alpha$ relatively to the z axis, whereas the states with energies E_{l-} have the spin pointing in the opposite direction at angle $2\theta_\alpha + \pi$ with the z axis.

The corresponding eigenvectors are

$$|\Psi_{l+}\rangle = \frac{1}{\sqrt{N}} \sum_n e^{il\theta_n} \begin{pmatrix} \cos \theta_\alpha \\ -e^{i\theta_n} \sin \theta_\alpha \end{pmatrix} |n\rangle, \quad (5)$$

$$|\Psi_{l-}\rangle = \frac{1}{\sqrt{N}} \sum_n e^{il\theta_n} \begin{pmatrix} e^{-i\theta_n} \sin \theta_\alpha \\ \cos \theta_\alpha \end{pmatrix} |n\rangle.$$

The velocity operator is given by $v_\theta = r\dot{\theta} = r \frac{i}{\hbar} [H, \theta]$,

$$v_\theta = -\frac{Va}{\hbar} \left\{ i \sum_{n,\sigma} c_{n\sigma}^\dagger c_{n+1\sigma} - \frac{V_\alpha}{V} \sum_{n,\sigma,\sigma'} [\sigma_r(\theta_{n,n+1})]_{\sigma\sigma'} c_{n\sigma}^\dagger c_{n+1\sigma'} + \text{H.c.} \right\}. \quad (6)$$

The velocity operator commutes with the Hamiltonian (1) and thus the eigenvectors of the velocity operator are the same $|\Psi_{l\pm}\rangle$ shown in Eq. (5), with the associated eigenvalues

$$v_{l\pm} = \frac{u_l + u_{l\pm 1}}{2} + \frac{u_l - u_{l\pm 1}}{2} \sqrt{1 + \tan^2 2\theta_\alpha}, \quad (7)$$

where $u_l = 2\frac{Va}{\hbar} \sin(2\pi l/N)$ is the velocity in the absence of the SOI.

It is helpful to introduce the tilt-spin operator $S_{2\theta_\alpha}$, defined like in the continuous ring model⁶

$$S_{2\theta_\alpha} = \cos 2\theta_\alpha S_z - \sin 2\theta_\alpha S_r, \quad (8)$$

which is a linear combination of S_z and S_r , the spin operators for z and radial directions, respectively. The tilt-spin operator also commutes with the Hamiltonian, it also has the eigenvectors $|\Psi_{l\pm}\rangle$, but associated with eigenvalues $\pm\hbar/2$.

In the absence of the SOI, all quantum states are fourfold degenerate, except those at the edges of the spectrum which are only twice degenerate.¹⁴ This can be seen in Fig. 1(a) where for $V_\alpha = 0$ the two branches E_{l+} and E_{l-} coincide. In this case $\theta_\alpha = 0$, the spin operator $S_{2\theta_\alpha}$ becomes S_z , and $|\Psi_{l\pm}\rangle$ become the $|\uparrow\rangle$ and $|\downarrow\rangle$ eigenstates of S_z . For $V_\alpha \neq 0$ the energy spectrum becomes broader (meaning that $|\max E_{l\sigma} - \min E_{l\sigma}|$ increases) and all states are twice degenerate since $E_{l\pm} = E_{-l\mp}$. To show this we marked by two horizontal lines the energies $E_{3-} = E_{-3+} = 1.839$ V and $E_{4+} = E_{-4-} = -0.0357$ V in Fig. 1(b).

In Fig. 2 we show the energy spectrum for an interval of Rashba energies V_α (in units of V). For all $V_\alpha \neq 0$ each line corresponds to double-degenerated states. For example, the thick lines describe the energies of the following paired states: $|-3+\rangle$ and $|3-\rangle$; $|-3-\rangle$ and $|3+\rangle$; $|0+\rangle$ and $|0-\rangle$. States at the crossing points in the spectrum shown in Fig. 2 preserve their fourfold degeneracy. Since the degenerate states for $V_\alpha \neq 0$ carry opposite currents $v_{l\pm} = -v_{-l\mp}$, but with opposite spins, the system can support a nonzero spin current.

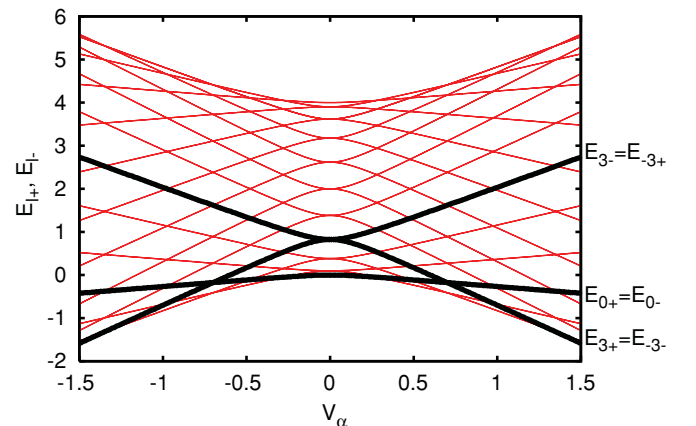


FIG. 2. (Color online) Spectrum of the 1D quantum ring with $N = 20$ points vs Rashba energy V_α . The eigenvalues $E_{3\pm}, E_{-3\pm}$ are marked with thick lines to illustrate the partial lifting of degeneracy when $V_\alpha \neq 0$. The energy unit is $V = \hbar^2/2m^*a^2$.

III. EFFECTS OF A TERAHERTZ PULSE

At $t = 0$ the quantum ring described above is exposed to a short terahertz two-component pulse

$$H_n(t) = Ae^{-\Gamma t} [\sin(\omega_1 t) \cos \theta + \sin(\omega_2 t) \cos n(\theta + \phi)] \quad (9)$$

of duration $\sim \Gamma^{-1}$ and amplitude A .¹⁴ $n = 1, 2$ describes the multipole order of the second component, while the phase difference ϕ between the two components makes the external perturbation asymmetric in space. The terahertz scale of the excitation frequencies $\omega_{1,2}$ is at least an order of magnitude larger than the spin relaxation rates in InAs semiconductor heterostructures which reaches values from anywhere between tens and hundreds of picoseconds.^{16,17}

The time evolution of the system's observables is determined by using the density operator $\rho(t)$, which at $t > 0$ satisfies a quantum Liouville equation

$$i\hbar \dot{\rho}(t) = [H + H_n(t), \rho(t)]. \quad (10)$$

Here the total Hamiltonian is interpreted as the many-body Hamiltonian of n_e noninteracting electrons. The initial condition is that $\rho(t = 0)$ represents the ground-state density operator which is constructed with the Slater determinant $\tilde{\psi}$ formed out by the wave functions $|\Psi_{l\sigma}\rangle$ shown in Eq. (5), corresponding to the n_e lowest-lying eigenstates of the initial time-independent Hamiltonian, Eq. (1):

$$\rho(t = 0) = |\tilde{\psi}\rangle\langle\tilde{\psi}|. \quad (11)$$

For any $t > 0$, Eq. (10) is solved numerically and $\rho(t)$ is obtained by using the Crank-Nicholson finite difference method¹³ with small time steps $\delta t \ll \Gamma^{-1}$. The expectation value of any observable O is then calculated as $\langle O \rangle = \text{Tr}[\rho(t)O]$.

The charge current around the ring is $I^c = ev_\theta$, while the azimuthal spin current corresponding to the spin projection along direction ν is $I_\nu^s = \frac{\hbar}{2}(\sigma_\nu v_\theta + v_\theta \sigma_\nu)$. As amply discussed in Refs. 6 and 8 this expression represents the fully symmetrized product between the velocity and spin operators, which in systems with SOI in general do not commute.

Since the spin operator $S_{2\theta_\alpha}$ (8) commutes with the unperturbed Hamiltonian (1), we calculate the expectation value of $I_{2\theta_\alpha}^s$ which corresponds to the direction of the spin $\mathbf{e}_{2\theta_\alpha} = \cos 2\theta_\alpha \mathbf{e}_z - \sin 2\theta_\alpha \mathbf{e}_r$. To simplify the notation we denote $I^s(t) = \langle I_{2\theta_\alpha}^s \rangle$, $v_\theta(t) = \langle v_\theta \rangle$, and $I^c(t) = ev_\theta(t)$. Since v_θ and $I_{2\theta_\alpha}^s$ commute with H , the charge and spin currents become constant after the external perturbation vanishes.

IV. NUMERICAL RESULTS

To illustrate our results we consider an InAs quantum ring of radius $r_0 = 14$ nm the electron effective mass being $m^* = 0.023m_e$. We choose our Rashba energy parameter $V_\alpha = 0.05$ (units of V), which corresponds to a SOI strength $\alpha = 37.56$ meV nm, within the range of experimentally determined values.¹⁸ The number of sites used in the discretization is $N = 20$, leading to a length unit of $a = 4.4$ nm and an energy unit of $V = 85.6$ meV. For a system with $n_e = 6$ electrons, in the many-particle noninteracting ground-state $\tilde{\psi}$, and for $V_\alpha = 0.05$ the occupied states are $|l\sigma\rangle = |0\pm\rangle$, $|1\pm\rangle$, and $|-1\pm\rangle$. In this configuration, that is, at $t = 0$, using Eq. (7)

one obtains the average velocity $v_\theta(t = 0) = 0$ and the spin current $I^s(t = 0) = 2\hbar(v_{0+} + v_{1+} + v_{-1+}) = -0.089Va/\hbar$.

The first external pulse we consider is the superposition of two dipoles corresponding to $n = 1$ in Eq. (9). For the selected parameters of the ring, in the absence of the SOI, we obtain the Bohr frequencies (given by $\omega_{l,l'} = |E_l - E_{l'}|/\hbar$) as $\hbar\omega_{0,1} = 2.89$ meV and $\hbar\omega_{1,2} = 8.60$ meV. In Figs. 3 and 4 we show the numerical results obtained for frequencies $\hbar\omega_1 = 2.83$ meV, $\hbar\omega_2 = 8.11$ meV, with the attenuation factor $\Gamma = 4\omega_1$, and amplitude $A = 67.68$ meV. The duration of the pulse is $t_f \approx 0.5$ ps. Since the pulse produces many-particle excited states, in our computation ω_1 and ω_2 are chosen to be slightly different from the obtained Bohr frequencies in an effort to create a more realistic algorithm that reproduces closely what happens in an experimental situation. Moreover, for ω_1 and ω_2 exactly equal to the Bohr frequencies the calculated results are similar.

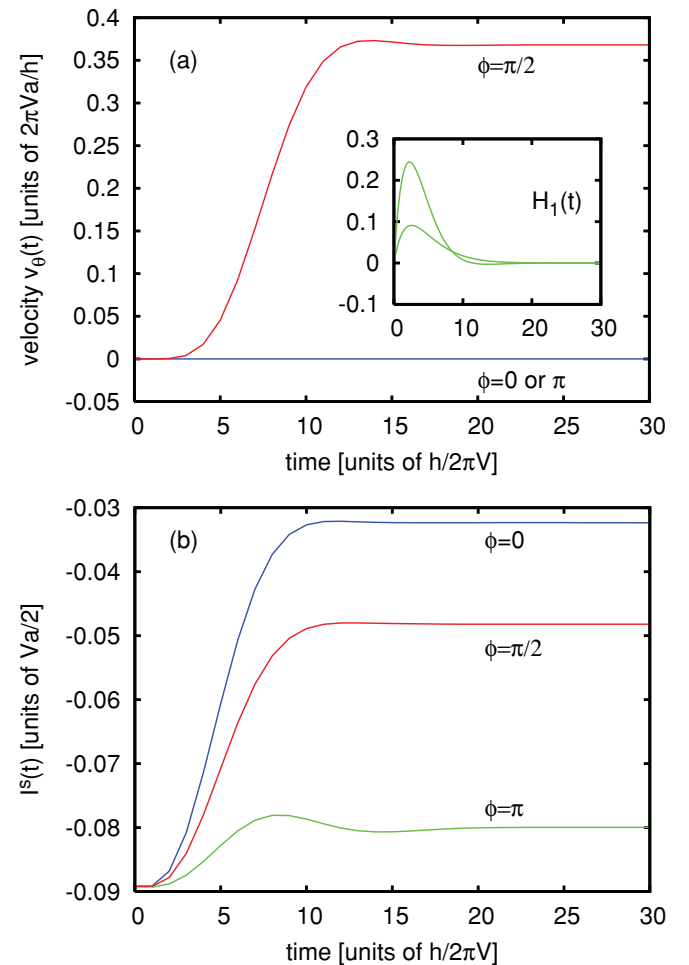


FIG. 3. (Color online) (a) The time evolution of the azimuthal velocity $v(t) = \langle v_\theta \rangle = I^c(t)/e$, (b) the spin current $I^s(t) = \langle I_{2\theta_\alpha}^s \rangle$ for the selected phase difference $\phi = 0, \pi/2, \pi$. The charge current is zero for both $\phi = 0$ and $\phi = \pi$, and thus in these cases a pure spin current is created. The inset shows the time dependence of the two components of the radiation pulse described by Eq. (9) with $n = 1$ for $\theta = \phi = 0$. The lower peak corresponds to the first term and the higher peak to the second term. The time unit is $\hbar/V = 0.0076$ ps.

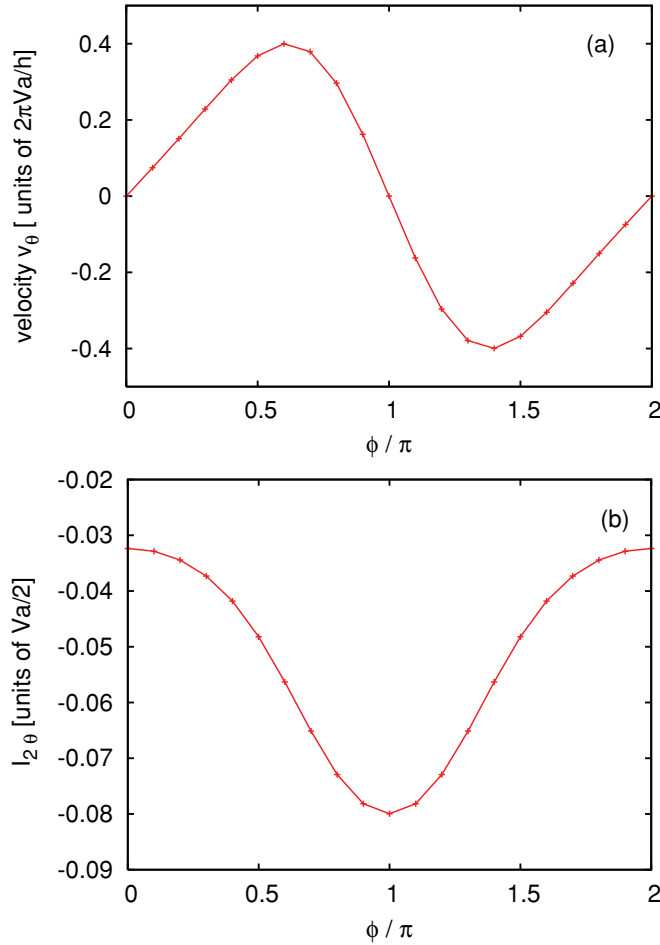


FIG. 4. (Color online) The stationary values of the velocity v_θ and spin current $I_{2\theta}^s$ after the external pulse vanishes (at $t \gg t_f$) vs the phase difference ϕ . The external pulse is $H_1(t)$, Eq. (9) with $n = 1$, i.e., a combination of two dipolar fields. The SOI parameter is $V_\alpha = 0.05$. Pure spin current, corresponding to zero charge current, is obtained when the phase difference ϕ is a multiple of π .

The time evolution of velocity $v_\theta(t)$ (proportional with the charge current) and that of the spin current $I^s(t)$ are illustrated in Fig. 3 for phase differences $\phi = 0, \pi/2$, and π . In Fig. 3(a) we recover the result of Ref. 13 where it was demonstrated that a charge current can be nonadiabatically generated through the application of a spatially asymmetric terahertz excitation. Thus, for $\phi = 0$, $v_\theta = 0$, while for $\phi = \pi/2$, $v_\theta \approx 0.37Va/\hbar$.

In Fig. 3(b) we present the time evolution of the spin current $I^s(t)$ corresponding to the spin projected on the proper axis $\mathbf{e}_{2\theta_\alpha}$. As previously stated, in the presence of SOI, the initial state of the system has a nonzero spin current, $I^s(0) \neq 0$. On account of the external pulse, the electrons in the ring are nonadiabatically excited, and the spin current evolves toward a new steady-state value. After the external pulse vanishes, the spin current $I_s(t)$ is constant in time, but its amplitude varies with the phase difference.

For a physical explanation of how the currents are generated one has to observe that the pulse described by Eq. (9) with $n = 1$, that is, two combined dipoles, creates along the circumference of the ring a sinusoidal angular potential with one maximum and one minimum. The amplitude of this sine

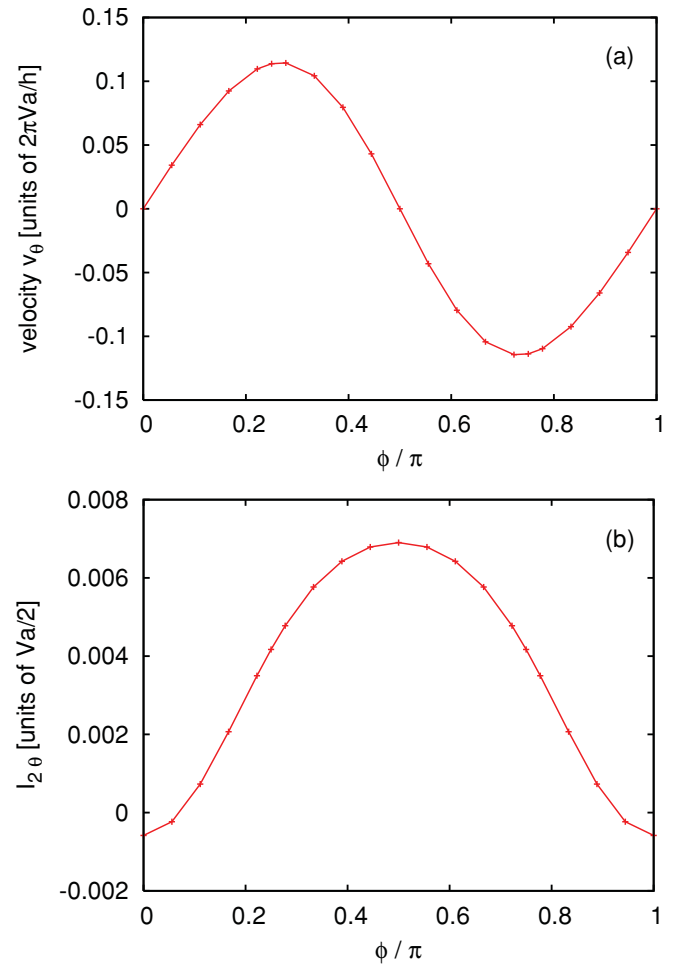


FIG. 5. (Color online) The stationary values of the velocity v_θ and spin current $I_{2\theta}^s$ after the external pulse vanishes (at $t \gg t_f$) vs the phase difference ϕ . The external pulse is $H_2(t)$, Eq. (9) with $n = 2$, i.e., a combination of a dipolar and a quadrupolar field. The SOI parameter is $V_\alpha = 0.05$. Pure spin current is now obtained when the phase difference ϕ is a multiple of $\pi/2$. The results are shown for $0 \leq \phi \leq \pi$ and they are identical for $\pi \leq \phi \leq 2\pi$.

wave first increases in time and then decreases and vanishes. When $\phi = 0$, that is, no spatial phase shift between the two components of the pulse, the maximum and minimum of the angular potential remain fixed in space, at $\theta = 0$ and $\theta = \pi$, respectively. In this case the combination of two dipolar components is equivalent to a single dipolar pulse. Charge current cannot flow in this situation because the velocities of electrons from the maximum to the minimum potential on both sides of the ring (i.e., through $\theta = \pi/2$ and through $\theta = 3\pi/2$) are opposite and cancel each other. However, spin current exists because the (average) spin orientations are also opposite on both sides following the velocity orientation and so the spin current on both halves of the ring have the same angular direction. Thus in order to generate a pure spin current a single dipolar pulse is sufficient. When $\phi \neq 0$ the sinusoidal potential is no longer fixed on the ring, but it rotates in time. An angular momentum is transferred to the electrons and charge current is created, in addition to the spin current.

The small oscillatory behavior of the current in Fig. 3, best seen at $\Phi = \pi$ when the spin current is at its lowest value, can be attributed to the damped oscillatory variation of the pulse in Eq. (9). The second term of the pulse, illustrated by the large peak in Fig. 3(a), becomes slightly negative around $t = 10$ units, creating a small oscillation both of the amplitude and of the rotation angle of the total potential on the ring, which is reflected in the currents.

We denote by v_θ and $I_{2\theta}$ the constant values of the velocity and spin current after the perturbation vanished [i.e., $v_\theta(t \gg t_f)$ and $I^s(t \gg t_f)$, respectively]. They are plotted as a function of the phase difference $\phi \in [0, 2\pi]$ in Fig. 4, but we note that they reflect the periodicity in ϕ of the applied pulse. For $\phi_{v1} = 1.89$ and $\phi_{v2} = 4.40$ (rad) the charge current is maximum and minimum, respectively, and the spin current has intermediate values. For ϕ equal to 0 and π no charge current flows through the ring ($v_\theta = 0$), whereas a spin current is present, $I_{2\theta} \neq 0$, being maximum for $\phi_{s1} = 0$ and minimum for $\phi_{s2} = \pi$. These are the critical phase differences angles for which only pure spin currents exist. In this case, the numerical results show that the states with opposite velocity, $|l+\rangle$ and $|l-\rangle$, are equally excited by the external pulse netting zero total velocity and no charge current in the steady state. This is not the case for intermediate angles where states with opposite velocity are asymmetrically excited and consequently generating nonzero values for both charge and spin currents.

In Fig. 5 we display v_θ and $I_{2\theta}$ obtained by exciting the system with a pulse given by Eq. (9) written for $n = 2$, which is a combination of a dipole and phase shifted quadrupole. The frequencies ω_1 , ω_2 , the attenuation factor Γ , and the amplitude A remain the same as in the previous case. Due to the quadrupolar component of the pulse, the period of v_θ and $I_{2\theta}$ is halved to $\Delta\phi = \pi$. The maximum and minimum values of v_θ are reached for $\phi_{v1} = 0.87$ and $\phi_{v2} = 2.27$ (rad). For the critical angles $\phi_{s1} = 0$ and $\phi_{s2} = \pi/2$ no charge current is induced in the ring ($v_\theta = 0$), but the induced spin current reaches extreme values, minima or maxima, respectively.

Again, in these situations only a pure spin current is induced in the ring.

V. CONCLUSIONS

In conclusion we studied the *nonadiabatic* excitation of spin and charge currents in a 1D quantum ring in the presence of Rashba SOI. The ring was subjected to an external pulse that is spatially asymmetric, having two components with an internal phase difference between them. We investigated two models, a dipole plus a rotated dipole and a dipole plus a rotated quadrupole. By numerical calculation we showed that for certain values of ϕ called ϕ_{v1} and ϕ_{v2} the induced charge current reaches extreme values with $I^c(\phi_{v1}) = -I^c(\phi_{v2})$. In the presence of the SOI, a nonzero spin current is always induced in the ring for both pulse models with amplitudes depending on the external parameters. We found critical values of the phase difference ϕ_{s1} and ϕ_{s2} for which the induced charge current disappears, whereas the spin current reaches maxima or minima. The method may be used in practice to convert an optical signal into a dissipationless (persistent) spin current for information transfer purposes. Similar results are obtained with the Dresselhaus SOI instead of Rashba SOI, due to the equivalence of the corresponding Hamiltonians. We also tested other parameters of the terahertz pulse (amplitude, frequencies, attenuation factor) and we obtained qualitatively similar results.

ACKNOWLEDGMENTS

This work was supported by the Icelandic Research Fund, DOE, Grant No. DE-FG02-04ER46139, Romanian PNCDI2 Research Programme (Grant No. 515/2009), and Core Programme (Contract No. 45N/2009). We acknowledge helpful discussions with Alexandru Aldea and Mugurel Ţolea. M.N. is thankful to Clemson University, Reykjavik University, and Science Institute - University of Iceland for their hospitality.

¹Y. A. Bychkov and E. I. Rashba, *J. Phys. C* **17**, 6039 (1984).

²G. Dresselhaus, *Phys. Rev.* **100**, 580 (1955).

³M. Büttiker, Y. Imry, and R. Landauer, *Phys. Lett. A* **96**, 365 (1983).

⁴L. Wendler, V. M. Fomin, and A. A. Krokhin, *Phys. Rev. B* **50**, 4642 (1994).

⁵T. Chakraborty and P. Pietiläinen, *Phys. Rev. B* **50**, 8460 (1994).

⁶J. Splettstoesser, M. Governale, and U. Zülicke, *Phys. Rev. B* **68**, 165341 (2003).

⁷S. Souma and B. K. Nikolić, *Phys. Rev. B* **70**, 195346 (2004).

⁸J. S. Sheng and K. Chang, *Phys. Rev. B* **74**, 235315 (2006).

⁹Q.-f. Sun, X. C. Xie, and J. Wang, *Phys. Rev. Lett.* **98**, 196801 (2007).

¹⁰G.-Y. Huang and L. Shi-Dong, *Europhys. Lett.* **86**, 67009 (2009).

¹¹M. Moskalets and M. Büttiker, *Phys. Rev. B* **68**, 075303 (2003).

¹²M. Moskalets and M. Büttiker, *Phys. Rev. B* **68**, 161311 (2003).

¹³V. Gudmundsson, C.-S. Tang, and A. Manolescu, *Phys. Rev. B* **67**, 161301 (2003).

¹⁴S. S. Gylfadóttir, M. Niță, V. Gudmundsson, and A. Manolescu, *Physica E* **27**, 278 (2005).

¹⁵F. E. Meijer, A. F. Morpurgo, and T. M. Klapwijk, *Phys. Rev. B* **66**, 033107 (2002).

¹⁶B. N. Murdin *et al.*, *Phys. Rev. B* **72**, 085346 (2005).

¹⁷K. C. Hall, K. Gündoğdu, E. Altunkaya, W. H. Lau, M. E. Flatté, T. F. Boggess, J. J. Zinck, W. B. Barvosa-Carter, and S. L. Skeith, *Phys. Rev. B* **68**, 115311 (2003).

¹⁸S. D. Ganichev *et al.*, *Phys. Rev. Lett.* **92**, 256601 (2004).